Volume 1 | Number 1 | Jan 2013 | Pages 1–100

## Nanoscale

www.rsc.org/nanoscale

ROYAL SOCIETY OF CHEMISTRY

This is an *Accepted Manuscript*, which has been through the Royal Society of Chemistry peer review process and has been accepted for publication.

*Accepted Manuscripts* are published online shortly after acceptance, before technical editing, formatting and proof reading. Using this free service, authors can make their results available to the community, in citable form, before we publish the edited article. We will replace this *Accepted Manuscript* with the edited and formatted *Advance Article* as soon as it is available.

You can find more information about *Accepted Manuscripts* in the **Information for Authors**.

Please note that technical editing may introduce minor changes to the text and/or graphics, which may alter content. The journal's standard **Terms & Conditions** and the **Ethical guidelines** still apply. In no event shall the Royal Society of Chemistry be held responsible for any errors or omissions in this *Accepted Manuscript* or any consequences arising from the use of any information it contains.

1    **High-yield nanosized (Si)AlPO-41 using ethanol polarity equalization and co-templating**
2    **synthesis approach**
3

4    Gerardo Majano[†], Kolio Raltchev[†], Aurelie Vicente[†], and Svetlana Mintova[†,*]

5

6    *†Laboratoire Catalyse & Spectrochimie, ENSICAEN - Université de Caen – CNRS,*
7    *6 boulevard du Maréchal Juin, 14050 Caen, France*
8
9
10    *Fax: + 33 (0)2 31 45 27 37 *E-mail: mintova@ensicaen.fr*
11

12

13    **Abstract**

14        Control of the crystallite dimensions of the microporous aluminophosphate AlPO-41

15    (AFO- type framework structure), and the Si-containing analogue SAPO-41, was attained

16    down to the nanometer scale under stable hydrothermal conditions. The combined application

17    of a tetraalkylammonium co-template (tetrapentylammonium hydroxide) along with an amine

18    structure directing agent (*n*-dipropylamine) stabilized through the use of ethanol in the initial

19    suspension enables a crystallization media, which remains homogeneous throughout the entire

20    synthesis. As direct consequence of the optimized homogeneity of the suspension, the AFO-

21    type microporous nanocrystals (AlPO-41 and SAPO-41) with a size in the range of 30-500

22    nm with yields surpassing 50% are obtained. The feasibility to obtain nanosized AlPO-41 and

23    SAPO-41 crystals using ethanol as a polarity equalizing agent, resulting in a scalable

24    hydrothermal synthesis from non-colloidal starting mixtures without the use of other assisting

25    methods is presented.

26

27

28    **1. Introduction**

29        In recent years, a whole plethora of applications have surged from the field of

30    nanosized microporous zeolites and metal-organic frameworks such as low-k layers, gas

31    sensors, separation membranes, composites, additives for diverse applications and catalytic

32    processes among many others.[1] This is mainly due to their nanosized dimensions and the

33    inherent characteristics that arise from shorter diffusion pathways, including better diffusion,

34    accessibility of the porous network and colloidal stability. A fairly mature field is particularly

35    found in the realm of zeolites, where numerous synthesis and modification approaches have

36    enabled the access to most of the known zeolite frameworks available in the nanoscale range.[2]

1      However, up to date microporous aluminophosphate materials (AlPOs), which replace

2      Si for P as basic framework building element,[3] have not followed suit. These materials, but

3      more precisely their Si-containing variety (SAPOs), are particularly interesting due to their

4      high temperature stability and neutral framework structures. Moreover the versatility of P and

5      its higher coordinative capacity extends the available zeolite frameworks and allows including

6      a wide variety of catalytically active metals. The latter aspect especially makes the fine-tuning

7      of the acidity more flexible compared with its aluminosilicate analogues. One promising

8      example is the dehydration of methanol, for which diverse SAPO-5, -11 and -41 materials

9      demonstrated to be good catalysts.[4] A more industrially relevant role is currently taken by

10     SAPO-34 (CHA), which is an active catalyst for the methanol-to-olefin (MTO) process

11     developed by UOP and Norsk Hydro, currently being implemented in diverse plants in

12     Nigeria and China.[5]

13     Generally AlPO materials are obtained with crystals in the micrometer range and only

14     some types were synthesized with nanosized dimensions with the help of complicated and

15     expensive experimental procedures.[6, 7] SAPO-34 was successfully obtained with a size of 100

16     nm starting from colloidal precursor suspension.[8] In addition, MnAlPO-5 was synthesized by

17     an ionic liquid media approach and its crystallization behavior was investigated.[9, 10] The

18     relevance of size control for any catalysts is widely known, but specifically for SAPO-11 the

19     positive effect of nanosized crystals has been demonstrated for their use as FCC additives by

20     increasing the yield up to 8.6 % .[11]

21     Unfortunately, owing to diverse intrinsic characteristics of AlPO crystallization, such

22     as the rather fast nucleation kinetics, its ionic nature and the tendency to form elongated

23     precursor structures, there is a tendency for the system to not only crystallize into large

24     crystals, but also to generally favor the crystallization of AlPO-5 (AFI) and AlPO-18 (AEI)

25     structures.[12] Thus mainly these and more dense frameworks such as AlPO-34 (CHA) have

26     been accessible as nanosized materials through traditional and non-traditional synthesis

27     methods. The known applied methods to manage crystal size listed above have relied on the

28     strict control of the crystallization time directing this way nucleation and limiting the rate of

29     crystallization.[6-12] However, as the long time stability of the medium, required for providing a

30     continuous and high-yield production of nanosized crystals, has not been studied.

31     A proven reliable strategy to obtain nanosized crystals, typically in aluminosilicate and

32     silicate precursor mixtures, consists of generating large amounts of nucleation sites by

33     increasing the amount of organic structure directing agent (SDA), which is accompanied by a

34     guaranteed high degree of homogeneity. Nevertheless, compared to zeolites, AlPO materials

1 also require the use of alkylamines as SDA, such as *n*-dipropylamine (DPA). Alkylamines

2 have a lower polarity than water and in large quantities they prove to decrease the level of

3 miscibility in the AlPO synthesis mixture. With developing the crystallization process, the

4 alkylamine is eventually protonated,[13] and the synthesis environment progressively becomes

5 more homogeneous.

6       Herein we present a synthesis approach for obtaining nanosized (Si)AlPO-41

7 (diameter of 15-500 nm) with a high colloidal stability and high crystalline yield by using

8 ethanol as a polarity equilibrating agent and tetrapentylammonium hydroxide as a co-template.

9 The synthesis is carried out under conventional hydrothermal conditions is stable,

10 reproducible and scalable.

11

12 **2. Experimental Part**

13 *2.1. AlPO-41 and SAPO-41 syntheses*

14       In a typical synthesis, *n*-dipropylamine (DPA, 99%, Aldrich) was added to aluminum

15 isopropoxide (AIP, > 98%, Aldrich). Then, if applicable, tetrapenthylammonium hydroxide

16 pentahydrate (TPeAOH, 20% in water, Aldrich) and, if applicable, absolute ethanol (EtOH,

17 AnalR NORMAPUR) was added and the mixture was stirred slightly. After this, deionized

18 water was added and the mixture was stirred for 30 min in a closed vessel until a complete

19 dissolution of AIP is achieved. The final precursor mixtures used for the synthesis of AlPO-

20 41 are summarized in Table 1. For the synthesis of SAPO-41, 0.1 a molar equivalent of

21 colloidal silica (Ludox AS-40, Aldrich) was then added drop wise (1 drop/5 sec, 500 rpm),

22 and the solution is stirred for additional 30 min. After this period, phosphoric acid (85%,

23 99.99%, Aldrich) was added drop wise to the mixture during stirring (1 drop/5 sec, stirring at

24 500 rpm). The addition of phosphoric acid was either automatic, using a dosing instrument or

25 controlled by hand (using the same rate). The composition of the final mixtures is given in

26 Table 1. Slightly milky but homogeneous starting suspensions were obtained using this

27 method. The aged mixtures (16 h) were put in a Teflon lined autoclave and heated at 180 °C

28 from 3 to 48 h in a conventional oven. The autoclaves were removed from the oven and

29 quenched. After hydrothermal treatment the samples were purified by centrifugation at

30 20000 rpm for 30 min and redispersed in water. The procedure was carried out three times

31 and the samples were freeze-dried prior further characterization.

32       The samples are named P (parent) for reference samples, AA (automatic addition) and

33 CA (controlled addition) referring to the method of phosphoric acid addition. The suffix for

1    the latter two specifies the synthesis time. Thus sample CA-24 h is a sample mixed using

2    controlled addition and hydrothermally treated for 24 h.

3

4    *2.2. Characterization*

5            Crystallinity of the samples was followed from quantitative powder XRD patterns

6    obtained using CuKα radiation in a PANalytical X'pert Pro diffractometer.

7            Scanning electron microscopy images for size and morphology evaluation were

8    obtained using a TESCAN Mira electron microscope at 30 kV.

9            Solid-state MAS NMR spectra of dry samples were carried out using a Bruker

10   ADVANCE    III-HD    Topspin    400    spectrometer    (9.4    T    at    10    kHz).

11   $^1$H-$^{31}$P CP MAS measurements were obtained with 3.5 ms of contact time, 0.1 M $H_3PO_4$ as

12   reference and $^1$H decoupling of 100 kHz, a cycle delay of 1 s and $^{27}$Al decoupling of 6 kHz.

13   For $^{27}$Al MAS NMR spectra a π/12 selective pulse was used, recycle delay of 0.5 s, and 0.1 M

14   $Al(NO_3)_3$ as reference.

15           Raman measurements were performed using a Labram 300 (Jobin Yvon) instrument

16   (He-Ne laser, 633 nm, gratings: 1800 lines/mm, 5 mW, acquisition time from 1-60 s)

17   equipped with a confocal microscope and a CCD detector.

18           Thermogravimetric measurements were carried out on a SETSYS SETARAM

19   instrument under a flow of atmospheric air (40 cm$^3$/min) and a heating rate of 5 °C/min.

20           The hydrodynamic diameters of the nanoparticles in water suspensions were

21   determined with a Malvern Zetasizer Nano. The back scattering geometry (scattering angle

22   173°, HeNe laser with 3 mW output power at 632.8 nm wavelength) allows measurements at

23   high sample concentration, since a complete penetration of the incident light through the

24   sample was not required.

25

26   **3. Results and discussion**

27   *3.1 Synthesis and evolution of the crystallization of (Si)AlPO-41 nanocrystals*

28           An aspect, which was ~~central~~ crucial to the conceptual development of the precursor

29   mixtures, was the homogeneity of the starting suspension. Thus diverse parameters were

30   optimized in order to successfully overcome it (see Table 1). Firstly, a basic

31   tetraalkylammonium hydroxide as a co-template is used. Solely the basicity of this kind of

32   compounds tends to increase the solubility of Al species. Preliminary experiments

33   demonstrated that TPeAOH was an effective co-template for obtaining AlPO-41, while the

34   use of tetramethylammonium hydroxide instead led to the formation of AlPO-31 and AlPO-5

1    (supplementary information, Fig. S1). Also, the sole addition of a co-template did not result in

2    a successful size diminution of the final crystals (Table 1, Fig. S2, sample P1). As a second

3    optimized parameter, the quantity of AIP was minimized as far as possible while increasing

4    the amount of $H_3PO_4$ (Table 1, sample P2). A final detail which was prioritized was the

5    addition of $H_3PO_4$, as is known to be critical for the entire synthesis. Thus the speed and

6    frequency of its addition was adjusted using an automatic dosing instrument. Dosing

7    parameters were chosen based on previous experience on synthesis of nanosized AlPO-34.[8]

8         Although the details explained above could be considered minimal, the focus of this

9    work was centered on the increase of the amount of DPA in the synthesis mixture for AlPO-

10   41 firstly (see Table 1). As a result an evident phase separation in the precursor mixture

11   before addition of the phosphoric acid was accompanied (Fig. 1a). This contra productive

12   behavior is most likely caused by the polarity difference between DPA and the water

13   environment. Although in their pure state these two solvents are clearly miscible, upon

14   dissolution of ionic species such as Al species, the system is no longer capable to sustain them,

15   due to the high concentration in the slurry, and the water coordination of the species

16   eventually causes a phase separation. During the AlPO synthesis, DPA in due course becomes

17   protonated,[13] and most likely homogenizes. Unfortunately it can be expected that this happens

18   after the initial formation of nuclei, thus the inhomogeneity contributes to the formation of a

19   suboptimal number of large nuclei. Therefore we chose ethanol as a polarity-equalizing agent

20   (5 P), as it possesses a polarity index between the one of water (10 P) and the one of DPA (~2

21   P). Thus it was used to replace water to the lowest known amount, which still enables AlPO

22   crystal formation, in order to promote optimal miscibility of the other two solvents. As can be

23   observed in photographs of the precursor mixtures, prior $H_3PO_4$ addition and after

24   hydrothermal synthesis, the synthesis environment remains homogeneous throughout the

25   entire process (Fig. 1a). After the synthesis, the product was obtained in the form of a

26   sedimented gel under clear liquid, which upon re-dispersion remains in colloidal form for

27   several days. The yields obtained were above 50 % and reached over 70 % in selected cases.

28   In general, the crystallization of AlPO-41, as monitored by XRD (Fig. 1b), is effectively

29   faster than most of the reported synthesis (1 *vs.* >2-5 d). AlPO-41 is present after 3 h synthesis

30   time. Nevertheless, the dominant phase at the early stages is AlPO-11, which disappears after

31   12 h. After 12 h hydrothermal treatment, only pure AlPO-41 phase is observed in the XRD

32   pattern.

33        The size evolution of the crystals synthesized under CA and AA conditions followed

34   by SEM (Fig. 2, left) show a rather straightforward development of the morphology already

1    presenting defined plate-like crystals between 80-500 nm after 12 h, a size which did not vary

2    strongly after 24-48 h. It is fairly well known that addition of phosphoric acid plays a critical

3    role for aluminophosphate synthesis to such extent that it even affects the final crystalline

4    phase and particle size. The use of automatic addition of phosphoric acid resulted in very

5    reproducible results. Nevertheless, after a certain period of phosphoric acid addition, a certain

6    agglomeration appeared and this affects the size of the crystals. The size of the crystals in

7    sample CA-24 24 h is a little smaller than in sample AA-24 h (see Fig. 2). Thus the synthesis

8    protocol was modified, and after the first observation of agglomeration of nanoparticles (after

9    ~75 % phosphoric acid was added) an additional period of 5-10 sec. stirring was applied in

10   order to avoid it as much as possible. A direct effect of this controlled addition protocol result

11   in a remarkable increase in homogeneity of the starting mixture and also in a decrease in the

12   final crystal size (Fig. 2, right). The evolution of the crystallinity of the samples obtained via

13   controlled synthesis protocol was almost identical to the ones obtained with the automated

14   approach (Fig. 3).

15      Additionally, the synthesis of SAPO-41 is performed via addition of colloidal silica

16   using the controlled addition method. The synthesis of SAPO-41 performed by adding the

17   silica prior the $H_3PO_4$ results in material with identical crystal sizes as shown in Fig. 4.

18   Moreover, the synthesis of SAPO-41 was performed with and without crystalline seeds (from

19   a CA-24 h synthesis) and no difference in the particle size and crystallinity was observed.

20   However, the morphology was more defined when 0.25 wt. % of seeds was added.

21      The size evolution observed in SEM imaging was also in line with DLS observation of

22   particles in the suspensions prior freeze drying (supporting information, Fig. S3). Although

23   the size distribution was rather broad, it still remain monomodal for all observed samples;

24   thus demonstrating the high degree of homogeneity. Comparing the crystalline samples (AA)

25   with the precursor synthesis mixture itself, it seems that the system undergoes an additional

26   dissolution from a mean particle size of 320 nm. The size decreases down to 114 nm after 12

27   h, when the dissolution ceases, the crystals start to grow again reaching a mean final size of

28   400 nm after 24 h.

29

30   *3.2 Physicochemical characterization of nanosized AlPO-41 crystals*

31      The nanosized AlPO-41, as evaluated by $^1$H-$^{31}$P CPMAS NMR, is chemically

32   identical to traditionally obtained materials (Fig. 5). The final product after 24 h was highly

33   crystalline as seen in the high definition of the spectra obtained, which upon deconvolution

34   revealed six phosphorous positions (at -20, -24, -28, -31, -32 and -36 ppm) and a small

1     shoulder at -17 ppm. The good definition of the signals was more evident with the peak at -28

2     ppm, which is usually not well resolved for AlPO-41. Although it is known that AlPO-41 has

3     only four crystallographic different sites, the presence of multiple signals in ^{31}P MAS NMR

4     has also been confirmed for highly crystalline samples.[14, 15] It may be feasible that the T1, T2

5     and T3 positions, which are accessible from the inside of the AlPO-41 channels, present

6     double signals due to the different coordination of DPA to P-O and Al-O sites. While the T4,

7     which is an internal position, would present a single weak signal due to lack of coordination

8     to the SDA. Furthermore, no signal related to $H_2PO_4^-$ defects at -11 and -14 ppm[14] can be

9     observed for all samples after 24 h. Moreover, by comparing both the AA-24 h and the CA-24

10    h samples, one can see broader signals in the latter case, which is related to the smaller

11    crystallite size. This signals, however, still showed a good resolution compared to other

12    samples in the literature. The coordination of P species also evolves as fast as the

13    crystallization process. Even in the case of the smallest AlPO-41 crystals (CA samples), the

14    organization occurs rapidly, as the defect sites located at -11 ppm at 6 h are no longer present

15    after 12 h synthesis time.

16        Some information about the SDA organization inside the crystalline and phosphorous

17    structures was obtained by Raman spectroscopy. Spectra of the AA samples, specifically

18    sample AA-24 h (Fig. 6), which are more detailed as the CA by virtue of their size, reveal that

19    the integrity of the SDA, predominantly DPA in its protonated form, is occluded into the

20    AlPO-41 network. This can be seen in the absence N-H signals of free DPA at 3330 cm$^{-1}$ in

21    all samples,[13] including one taken after only 3 h crystallization time. Typical C-H stretch

22    bands of the occluded SDA in AlPO-41 between 2750 cm$^{-1}$ and 3200 cm$^{-1}$ are already present

23    after only 3 h,[16, 17] and are shifted to higher wavenumbers compared to the pure DPA. The

24    relative intensity of these bands expectedly varies with progressing crystallization. Namely,

25    the central vibration at 2947 cm$^{-1}$ decreases and splits with time, while the one at 2909 cm$^{-1}$

26    almost disappears after 24 h. Other vibrations, including the $CH_3$ deformation at 1459 cm$^{-1}$

27    and 1452 cm$^{-1}$, P-O stretching at 1092 cm$^{-1}$, and T-O-T bending vibrations at 491 cm$^{-1}$ and

28    285 cm$^{-1}$ can be seen as already well defined after 3 h. It should be remarked that no visible

29    change could be observed due to the inclusion of $TPeA^+$, most likely due to the small amount

30    used and its structural similarity to the $DPA^+$.

31        Finally, it has been previously suggested that ethanol can promote AlPO-41

32    crystallization.[18] Nevertheless, with our current spectroscopic results we can neither confirm

33    or refute this effect.[19] The strong similarity of the C-H vibrations for ethanol and DPA, which

34    appear in the region of 2500-3000 cm$^{-1}$, does not allow distinguishing between them.

1        Taking these results into account, it is reasonable to expect firstly, that the

2    coordination of $DPA^+$ in the network of AlPO-41 does not vary with higher content from the

3    typically observed positions. Additionally, $TPeA^+$ seems to either be in a conformation close

4    to the one of $DPA^+$ or the quantity used is too small, and therefore is overlapped by the

5    signals of $DPA^+$. As DPA is known to be an unspecific SDA for different frameworks, this

6    further supports the expected role of TPeAOH as both an additional help in increasing the

7    solubility of Al species and providing a stronger structure direction for the AlPO-41

8    formation. This is especially relevant taking into account that quaternary ammonium species

9    are stronger SDAs under the polarity of aqueous media. Concerning the role of ethanol in the

10   synthesis, there is only one reference in the open literature of being used as a solvent in AlPO-

11   n synthesis.[18] Nevertheless, in the aforementioned case the synthesis was applied from a

12   dense gel and the quantity of ethanol was comparatively small. Although it is evident that the

13   authors obtained micron-sized AlPO-41 by filtration, no size effects were reported. In our

14   case the effect of ethanol can safely be attributed to the polarity equalizing effect as a solvent.

15   This facilitates the miscibility of water and DPA and guarantees a solubility of all precursor

16   species at the same time.

17       As the presented approach entails using the addition of ethanol and the substitution of

18   only 6% of the original amine template by TPeAOH, it remains economical. The simple and

19   facile nature of the approach also enabled the synthesis to be consistently scaled up, from a

20   conventional volume for research of 20 mL up to 250 mL synthesis mixtures, with no

21   observable changes in crystalline phase obtained, crystal size or yield. Furthermore, the

22   synthesis remained completely reproducible. This is a hopeful sign that the synthesis

23   approach has a good prospect to be scaled up further.

24

25

26   **4. Conclusions**

27       The synthesis of nanosized AlPO and related materials, including SAPO and MAPO

28   structures, continues to be a veritable challenge worth pursuing for current and future

29   catalysis and sorption applications. We have demonstrated the possibility of obtaining

30   nanosized (Si)AlPO-41 material, from a concentrated precursor environment that is stable

31   during the extended time at hydrothermal conditions. With a minimal use of

32   tetrapenthylammonium hydroxide pentahydrate (TPeAOH) as co-template and ethanol as co-

33   solvent, this method may facilitate new venues for the effective control of the crystal size of

34   AlPO materials, which greatly influences the functional features for catalysis and sorption.

1     Beyond this result, it was also possible to reasonably scale up the synthesis without

2     compromising any of the properties of the material. Another interesting fact was that, as far as

3     we were able to observe, in the initial stages of crystallization, the AlPO-11 side phase was

4     also present as nanosized crystals, allowing safely speculating that the polarity equalization

5     approach may be transferable to other AlPO- type framework structures. Taking into

6     consideration that the synthesis environment of the former is more ionic, the synthesis

7     approaches studies should be more specialized for AlPO materials and further studies into the

8     variation of the polarity of the solvent would contribute to future synthesis research.

9

12

13     References
14

15     1.     L. Tosheva and V. P. Valtchev, *Chem. Mater.*, 2005, **17**, 2494-2513.

16     2.     S. Mintova, J.-P. Gilson and V. Valtchev, *Nanoscale*, 2013, **5**, 6693-6703.

17     3.     S. T. Wilson, B. M. Lok, C. A. Messina, T. R. Cannan and E. M. Flanigen, *J. Am.*
18     *Chem. Soc.*, 1982, **104**, 1146-1147.

19     4.     W. Dai, W. Kong, G. Wu, N. Li, L. Li and N. Guan, *Catal. Commun.*, 2011, **12**, 535-
20     538.

21     5.     G. A. Olah, A. Goeppert and G. K. S. Prakash, in *Beyond Oil and Gas: The Methanol*
22     *Economy*, Wiley-VCH Verlag GmbH & Co. KGaA, 2009, ch. 13, pp. 279-288.

23     6.     H. Du, M. Fang, W. Xu, X. Meng and W. Pang, *J. Mater. Chem.*, 1997, **7**, 551-555.

24     7.     S. Mintova, S. Mo and T. Bein, *Chem. Mater.*, 1998, **10**, 4030-4036.

25     8.     H. van Heyden, S. Mintova and T. Bein, *Chem. Mater.*, 2008, **20**, 2956-2963.

26     9.     E.-P. Ng, S. S. Sekhon and S. Mintova, *Chemical Communications*, 2009, 1661-1663.

27     10.     E.-P. Ng, L. Itani, S. S. Sekhon and S. Mintova, *Chem. - Eur. J.*, 2010, **16**, 12890-
28     12897.

29     11.     L. Han, Y. Liu, F. Subhan, X. Liu and Z. Yan, *Micropor. Mesopor. Mater.*, 2014, **194**,
30     90-96.

31     12.     S. Oliver, A. Kuperman and G. A. Ozin, *Angew. Chem. Int. Ed.*, 1998, **37**, 46-62.

32     13.     B. Han, C.-H. Shin, P. A. Cox and S. B. Hong, *J. Phys. Chem. B*, 2006, **110**, 8188-
33     8193.

34     14.     M. Hartmann, A. M. Prakash and L. Kevan, *J. Chem. Soc. Faraday Trans.*, 1998, **94**,
35     723-727.

1    15.    R. M. Kirchner and J. M. Bennett, *Zeolites*, 1994, **14**, 523-528.

2    16.    M. Rokita, M. Handke and W. Mozgawa, *J. Mol. Struct.*, 2000, **555**, 351-356.

3    17.    A. C. Gujar, A. A. Moye, P. A. Coghill, D. C. Teeters, K. P. Roberts and G. L. Price,

4           *Micropor. Mesopor. Mater.*, 2005, **78**, 131-137.

5    18.    H. W. Clark, W. J. Rievert and M. M. Olken, *Microp. Mat.*, 1996, **6**, 115-124.

6    19.    Y. Yu, K. Lin, X. Zhou, H. Wang, S. Liu and X. Ma, *J. Phys. Chem. C*, 2007, **111**,

7           8971-8978.

8

9

10

1    **Table 1.** Overview of initial compositions used for synthesis of selected samples (P: parent,

2    AA: automatic addition, CA: controlled addition) and their particle size.

3

| Sample | Conditions | Composition | Size (nm)[a] |
|---|---|---|---|
| P1 | 24 h | $2Pr_2NH: 1Al_2O_3: 1P_2O_5: 40H_2O$ | 1000 |
| P2 | 24 – 72 h | $3Pr_2NH: 0.7Al_2O_3: 1.3P_2O_5: 50H_2O$ | 1200[b] |
| P3 | 24 h | $2.8Pr_2NH: 0.2TPeAOH: 0.7Al_2O_3: 1.3P_2O_5: 50\ H_2O$ | 1200 |
| AA | 3 – 48 h | $2.8Pr_2NH: 0.2TPeAOH: 0.7Al_2O_3: 1.3\ P_2O_5: 25\ EtOH: 25\ H_2O$ | 300-500 |
| CA | 6 – 48 h | $2.8Pr_2NH: 0.2TPeAOH: 0.7Al_2O_3: 1.3\ P_2O_5: 25\ EtOH: 25\ H_2O$ | 30-200 |
| Si-CA | 24 h | $2.8Pr_2NH: 0.2TPeAOH: 0.7Al_2O_3: 1.3P_2O_5:$ $0.1SiO_2: 25EtOH: 25\ H_2O$ | 60-200 |

4    [a]average crystal size based on SEM and DLS characterization, [b]layered product.

5

6

7

8

9

10

11

12

13

14

15

16

17

18

19

20

21

22

23

24

25

26

27

28

29

1   **Figures**

2

3
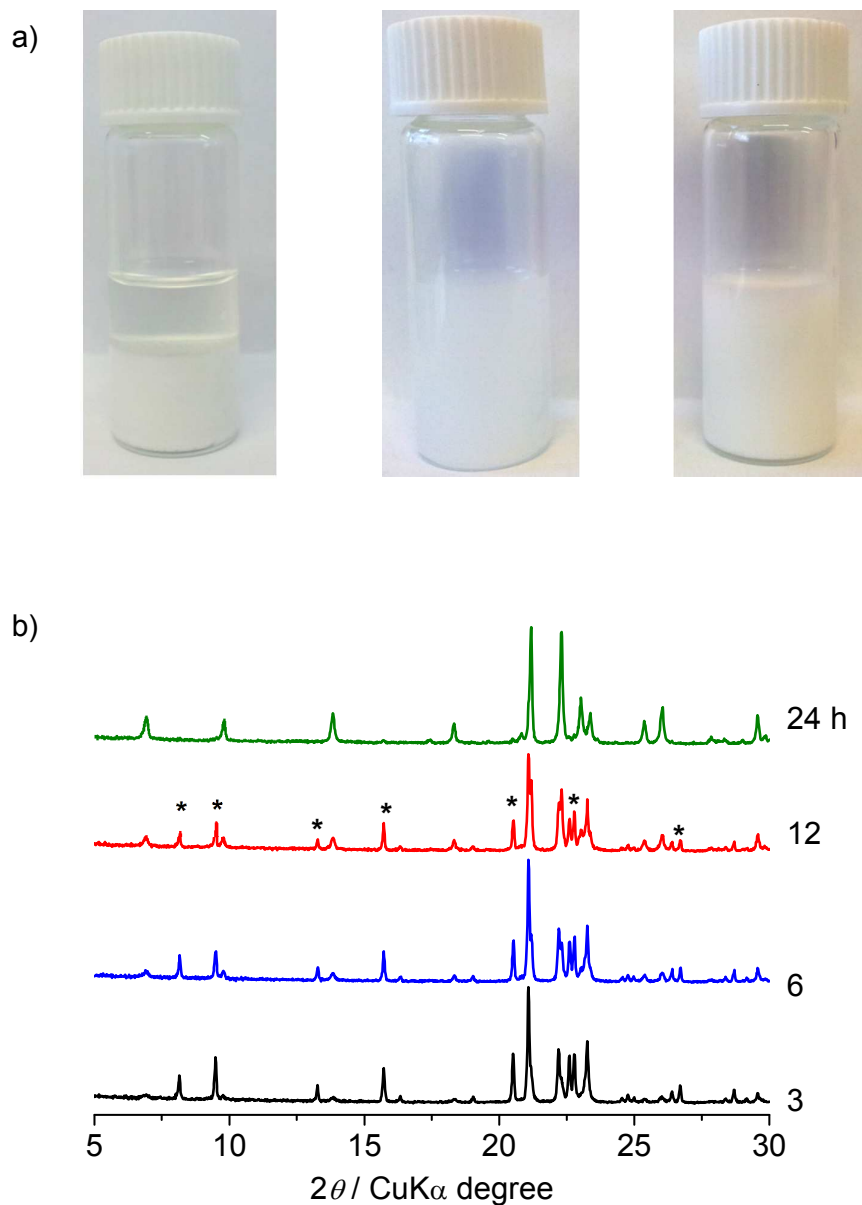


**Figure 1.** (a) Photographs of precursor mixtures for conventional AlPO-41 (sample P1, left) and ethanol and TPeAOH containing mixture (middle) before addition of the phosphoric acid, and final colloidal suspension of crystalline nanosized AlPO-41 (sample AA, right); (b) Crystallinity evolution of samples synthesized under automated addition of phosphoric acid (samples AA) monitored by XRD after different synthesis times (3 to 24 h).

**Automatic addition**                    **Controlled addition**

6 h

12 h

24 h
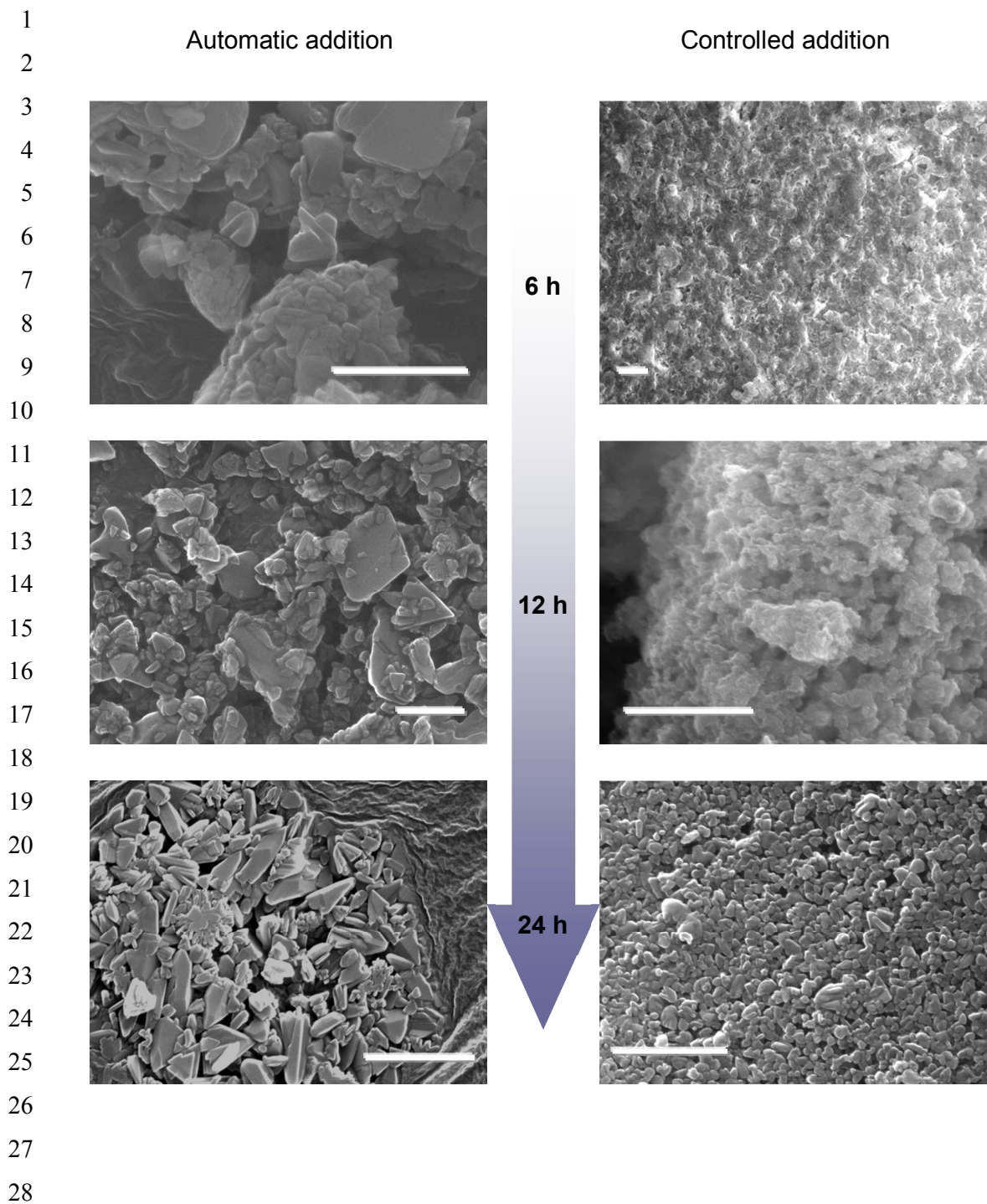
**Figure 2** Scanning electron microscopy images depicting the size and morphology evolution of particles during the synthesis carried out with automatic addition AA-6 to 24 h (left) and controlled addition CA-6 to 24 h (right) of phosphoric acid (scale bar M= 1 μm).
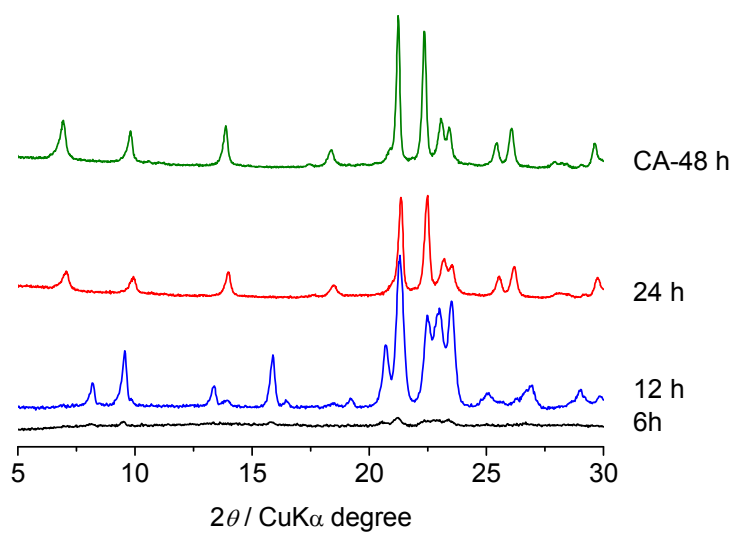
**Figure 3**. Crystallinity evolution of AlPO-41 samples prepared under controlled mixing (samples CA) monitored by XRD after different synthesis time (6 to 48 h).

1
2
3
4
5
6
7
8
9
10
11
12
13
14
15
16
17
18
19
20
21
22
23
24
25
26



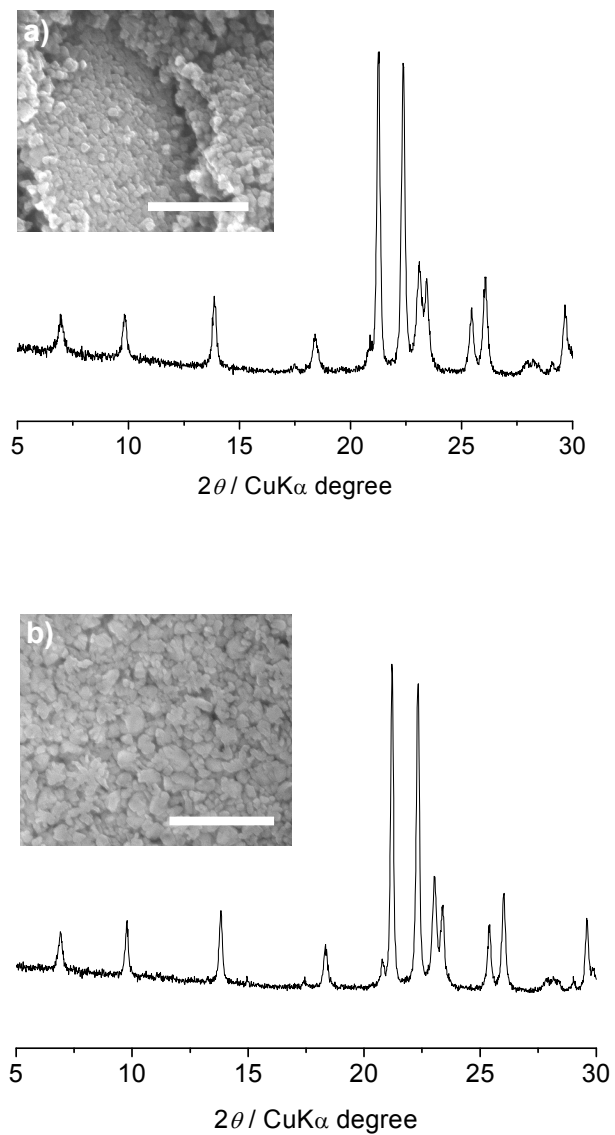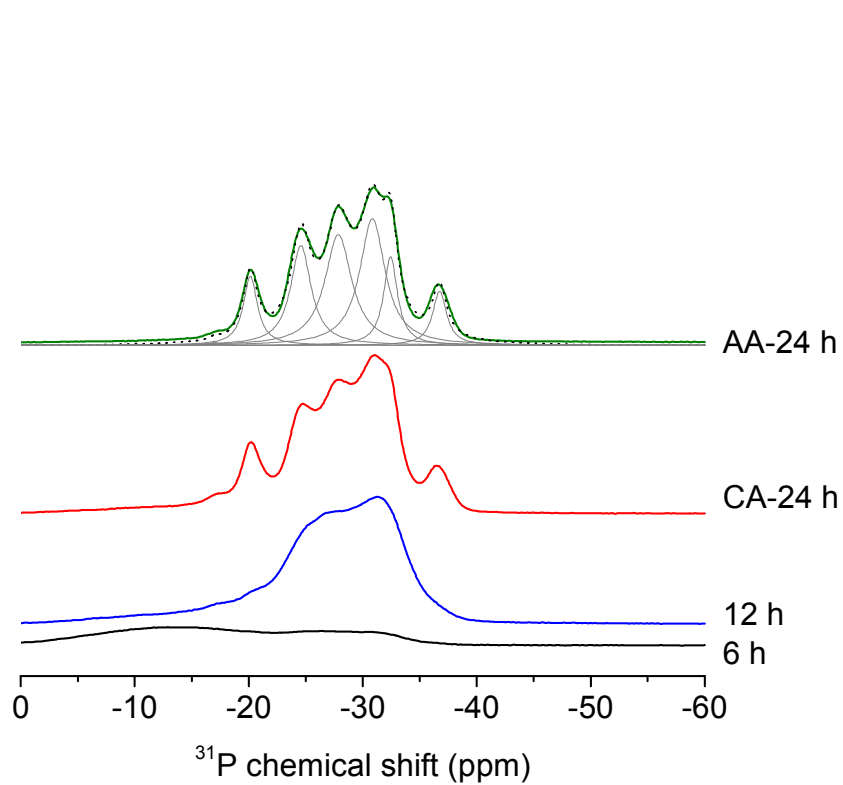27    **Figure 4**. XRD patterns and SEM images (insets, scale bar M = 1 μm) of nanosized SAPO-41

28    samples obtained using the ethanol equalization approach synthesized with (a) 1 wt. % AlPO-

29    41 seeds and (b) without AlPO-41 seeds.

30
31
32
33
34

1
2
3
4
5
6
7                                                                                    AA-24 h
8
9
10                                                                                   CA-24 h
11
12
13                                                                                   12 h
                                                                                     6 h
14     0      -10     -20     -30     -40     -50     -60
15                        $^{31}$P chemical shift (ppm)
16
17
18
19
20     **Figure 5.** $^{1}$H-$^{31}$P CPMAS NMR spectra of AlPO-41 samples in advanced stages of
21     crystallization from 6 to 24 h obtained by automated (AA-24 h) and controlled (CA-24 h)
22     methods. Deconvoluted fit for sample AA-24h as dashed line.
23
24
25
26
27
28
29
30
31
32
33
34

**Nanoscale Accepted Manuscript**

1
2
3
4
5
6
7
8
9
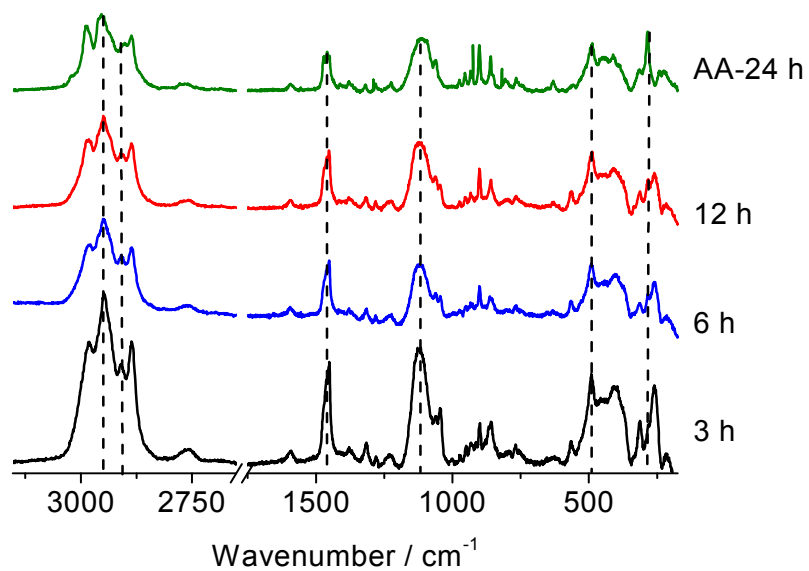10
11
12
13
14
15
16



17 **Figure 6.** Raman spectra of AlPO-41 samples synthesized by automated method (sample AA:

18 3 to 24 h).